

Improved Semi-Empirical Method for Power-On Base-Drag Prediction

F. G. Moore*

Aeroprediction, Inc., King George, Virginia 22485

and

T. C. Hymer†

U.S. Naval Surface Warfare Center, Dahlgren, Virginia 22448

Improved methods for base-pressure prediction under base-bleed and rocket motor-on conditions have been deployed. The base bleed method makes several refinements to the method developed by Danberg at the Army Research Laboratory in Aberdeen, Maryland. The improved rocket motor-on, base-pressure prediction improves upon the method developed at the Army Missile Command in Huntsville, Alabama, by Brazzel and some of his colleagues. The major refinement to the base bleed method of Danburg was to estimate the power-off value of base pressure empirically based on an extensive database, as opposed to using computational fluid dynamics codes to predict this term. The major modifications to the power-on base-pressure prediction method of Brazzel was to extend its range of applicability to high values of thrust coefficient, to Mach numbers less than 1.5, and to different afterbody shapes. In comparing the improved methods for power-on base-drag prediction to experiment, it was seen that both methods gave reasonable agreement to most experimental databases.

Nomenclature

A_{ref}	=	reference area, which is a cross-sectional area of body, ft ²
A_t	=	area of rocket motor nozzle throat cross section, ft ²
C_A	=	axial-force coefficient
C_{AB}, C_{Af}	=	base, skin-friction, and wave components of axial-force coefficient, respectively
C_{PB}	=	base-pressure coefficient
C_T	=	thrust coefficient
d	=	diameter, ft
I	=	nondimensional base-bleed injection parameter
M	=	Mach number
\dot{m}	=	mass rate of flow, ρAV
P	=	static pressure, lb/ft ²
P_0	=	total pressure, lb/ft ²
T	=	temperature, °R, or thrust, lb
V	=	velocity, ft/s
x_j	=	distance of jet exit from body base (positive behind base)
α	=	body angle of attack, deg (positive nose up)
γ	=	ratio of specific heats
θ	=	jet exit angle, boattail or flare angle
ρ	=	density, slugs/ft ³

Subscripts

B	=	conditions at body base
C	=	conditions in rocket motor chamber
j	=	conditions at nozzle exit
r, ref	=	reference conditions
∞	=	freestream conditions

Superscript

* = indicates conditions where $M = 1.0$

Introduction

THE present approach to predict the effect of the rocket engine burning on the base drag of weapons was integrated into the aeroprediction code in the late 1970s and has not been upgraded since that time. The method used was basically an extension of the Brazzel^{1,2} technique. The Brazzel technique was for solid rockets, which had an exit Mach number of 1.0 or greater. The technique required knowledge of some of the details of the rocket such as chamber pressure, exit area to nozzle throat area, specific heat ratio of the exit gas, and location of the nozzle exit with respect to the base of the missile or projectile. This approach has been shown to give reasonable estimates of power-on base drag for a limited range of flight conditions when these parameters (P_C/P_∞ , A_j/A_t , γ_j , x_j/d_r) are known.

Although the approach by Brazzel has its strengths, it also has several weaknesses when approached from an aerodynamics viewpoint. First, it was limited to jet momentum flux ratios (RMF) of about 2.5 or less. Many of the world's rockets have values of this parameter much higher and therefore the method of Brazzel needs extending to higher values of RMF. This was done and documented informally many years ago but has never been documented formally. The recent book² by the first author documents the modified Brazzel technique in an abbreviated fashion. This paper will serve as formal documentation of the extension of the Brazzel method to higher values of RMF. Another problem with the Brazzel technique from an aerodynamicist's viewpoint is the required knowledge of the engine parameters. These parameters are required in order to perform conceptual design tradeoffs of various rockets for total drag when the engine is burning. As a result of this desire for conceptual trade studies where some account of engine-on base drag is considered, other simplified procedures are needed for base-drag prediction. This paper will address two other options to calculate power-on base drag. Another limitation of the Brazzel method is its limitation to supersonic flow at the nozzle exit. Although the exit supersonic flow requirement is not a severe limitation for most rocket engines, it is a severe limitation for projectile configurations that use base bleed for base-drag reduction. As a result of this shortcoming, a method developed by Danberg³ for predicting base drag for small values of the bleed injection parameter I will be made more general. A final limitation of the Brazzel method is that it was derived based on

Received 11 December 2000; revision received 3 August 2001; presented as Paper 2001-4328 at the Atmospheric Flight Mechanics Conference, Montreal, QC, Canada, 6–9 August 2001; accepted for publication 8 August 2001. This material is declared a work of the U.S. Government and is not subject to copyright protection in the United States. Copies of this paper may be made for personal or internal use, on condition that the copier pay the \$10.00 per-copy fee to the Copyright Clearance Center, Inc., 222 Rosewood Drive, Danvers, MA 01923; include the code 0022-4650/02 \$10.00 in correspondence with the CCC.

*President, 9449 Grover Drive, Suite 201. Associate Fellow AIAA.

†Aerospace Engineer, Missile Systems Division, Weapons Systems Department, Dahlgren Division. Member AIAA.

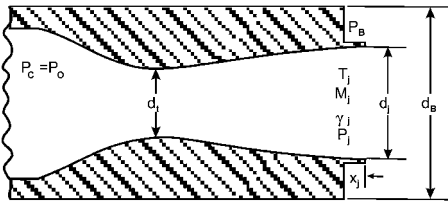
freestream Mach number data of 1.5 and greater. It therefore needs to be extended to at least the transonic Mach-number regime.

It is the purpose of this paper to develop the methodology to overcome the shortcomings of both the Brazzel and Danberg methods for predicting power-on base-pressure coefficient. The modifications to the Brazzel^{1,2} and Danberg³ methods will be incorporated into the aeroprediction code for power-on base drag prediction and be a part of the next release to the public, which will be in 2002 (AP02). The power-on base-drag modifications will also be incorporated into the personal computer interface for the AP02 so as to allow the various power-on options to be considered in a very user-friendly mode.

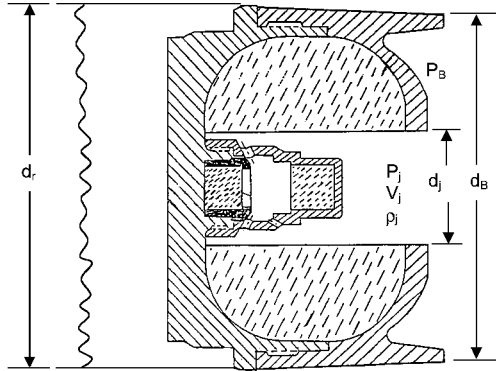
Analysis

Power-On Base Drag for $M_j \geq 1.0$

Because the power-on base drag prediction method of the aeroprediction code is based on an extension of the method of Brazzel and colleagues^{1,2} it is appropriate to briefly summarize Brazzel's



a) Rocket engine parameters



b) Typical projectile base bleed configuration³

Fig. 1 Nomenclature for power-on conditions for rockets and base-bleed concepts.

method. Figure 1a shows the nomenclature that is used for the rocket engine parameters. The Brazzel and Henderson method defines the base pressure as

$$\frac{P_B}{P_\infty} = 0.047(5 - M_\infty) \left[2 \left(\frac{x_j}{d_B} \right) + \left(\frac{x_j}{d_B} \right)^2 \right] + \left(\frac{T_j}{T_j^*} \right) \left[0.19 + 1.28 \left(\frac{\text{RMF}}{1 + \text{RMF}} \right) \right] \left[\frac{3.5}{1 + 2.5(d_B/d_r)^2} \right] \quad (1)$$

where

$$\text{RMF} = \frac{\gamma_j P_j d_j^2 M_j^2}{\gamma_\infty P_\infty d_r^2 M_\infty^2} \quad (2)$$

$$\frac{T_j}{T_j^*} = \frac{(\gamma_j + 1)/2}{1 + [(\gamma_j - 1)/2] M_j^2} \quad (3)$$

where x_j/d_B is the distance the nozzle exit extends past the base in calibers.

Brazzel's method was built around two fundamental assumptions that he was able to develop based on analysis of experimental data for jet exit Mach numbers 1.0–3.8. The first assumption is that freestream Mach number and nozzle diameter are accounted for by the momentum flux term defined by Eq. (2). The second assumption was that jet exit Mach number could be described by the ratio of the jet static temperature for a given jet Mach number to that at a jet exit Mach number of 1.0. This relationship is defined by Eq. (3).

In reality, the Brazzel method was geared primarily to accounting for base drag for sustainer rocket motors that typically have values of thrust coefficient of 0.2 to about 3.0 and fly supersonically. However, as the mass flow ratio or thrust coefficient get large or the freestream Mach number is transonic the Brazzel method produces increasingly erroneous results for many cases. This behavior of Eq. (1) is illustrated in Fig. 2, which correlates base-pressure predictions on a cylindrical afterbody for a jet exit Mach number of one ($T_j/T_j^* = 1.0$). The Brazzel correlation fits the data taken from Refs. 1, 4–6 quite nicely for RMF values up to almost 0.5. Above values of 0.5, the data of Fig. 2 are more scattered, particularly for RMF values above about 1.5.

Brazzel indicated he had little data for high thrust ratios to use in the method development. The method of Refs. 2 and 7, and included in the AP98 (Ref. 8), uses the method of Brazzel for RMF values up to 1.5 and then the empirical curve fits that bracket most of the data of Fig. 2 in terms of upper and lower values along with a

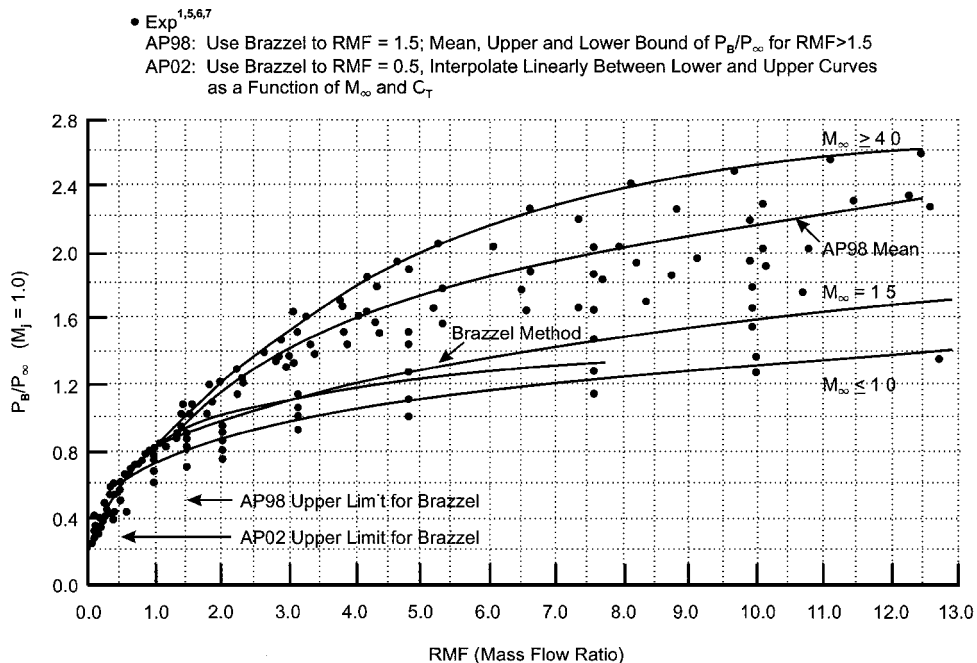


Fig. 2 Correlation of average base pressure for some conditions at exit.

mean value. The mean value of base-pressure coefficient between the lower and upper values of P_B/P_∞ as RMF gets larger is shown in Fig. 2. However, in examining the data of Fig. 2 more closely it was found that for higher values of C_T , P_B/P_∞ was primarily dependent on freestream Mach number with little dependence on jet exit Mach number or jet exit diameter. Apparently for high thrust levels such as would occur on a high impulse sustainer or a booster rocket motor, one of the main correlation parameters for P_B/P_∞ is M_∞ . Thus, the AP02 will modify the current methodology for power on base-drag prediction of Ref. 7 for RMF values greater than 0.5 so that P_B/P_∞ will be correlated with freestream Mach number, as opposed to giving the user an upper, lower, and mean value of P_B/P_∞ for all freestream Mach numbers. The discussion of power-on base-drag prediction will thus be broken down by thrust or momentum flux ratio level.

We will first of all consider the lower values of RMF or C_T that are more representative of a lower thrust sustainer engine. For these values of RMF, we will use the Brazzel method given by Eqs. (1–3). To utilize the Brazzel method, we therefore must obtain values of RMF either through direct input or through calculation based on known engine quantities. The parameters that are normally known in a rocket engine are the chamber pressure P_C , the nozzle throat and exit area, and the ratio of specific heats for the gas of interest. We can use this information to determine the quantities M_j and RMF through the following process. We will first assume isentropic flow throughout the nozzle. Isentropic flow means there are no strong shock waves in the nozzle, only weak expansion or compression waves. Lack of shock waves in the nozzle means that the chamber pressure, which is the total pressure because velocity is zero in the chamber, is constant throughout the nozzle. Then, using this information, along with isentropic flow relations for flow through a nozzle, the jet exit Mach number and pressure relationships can be defined. The reader is referred to Ref. 9 for the details of this process. Reference 9 documents the methods discussed in this paper in more detail and also gives more example cases as well.

Now knowing P_j/P_∞ , A_j/A_{ref} , M_j/M_∞ , and γ_j/γ_∞ , we can compute the jet momentum flux ratio from Eq. (2). Finally, knowing x_j/x_B as a defined physical parameter and T_j/T_j^* from Eq. (3) the base-pressure ratio for power on can be computed from Eq. (1).

The base-pressure coefficient is defined by

$$C_{P_B} = (2/\gamma M_\infty^2)(P_B/P_\infty - 1) \quad (4)$$

where P_B/P_∞ comes from Eq. (1). Finally, the base-drag coefficient for power-on conditions is

$$C_{A_B} = -C_{P_B}[(d_B/d_r)^2 - (d_j/d_r)^2] \quad (5)$$

Also notice that Eq. (5) subtracts out that part of the base area attributed to the jet exit diameter, where the pressure is P_j , not P_b . P_j is used in the calculation of jet thrust coefficient through the relationship

$$C_T = 2 \text{RMF} + (d_j/d_r)^2 (2/\gamma_\infty M_\infty^2)(P_j/P_\infty - 1) \quad (6)$$

RMF and P_j/P_∞ of Eq. (6) come from Eq. (2) and the isentropic flow relationships discussed earlier and defined in more detail in Ref. 9. The total axial-force coefficient is then

$$C_A = C_{A_W} + C_{A_f} + C_{A_B} - C_T \quad (7)$$

As mentioned earlier, Eq. (1) is limited to low to moderate values of jet momentum flux ratio ($\text{RMF} \leq 0.5$). Many rockets, including some in the U.S. Navy, have values of RMF much higher than 0.5. As a result, the method of Brazzel and Henderson¹ was extended to higher values of RMF using data later taken by Craft and Brazzel,⁴ Henderson,⁵ and Deep et al.⁶

The method that will be a part of the AP02 will therefore have several changes from that in the AP98. First, the method of Brazzel will be used up to values of RMF of 0.5 vs 1.5 as currently done in the AP98. Next, for values of RMF > 0.5 a more robust empirical relationship was derived for P_B/P_∞ than Eq. (1). This empirical relationship was based on Eq. (1), but extended Eq. (1) to more

Table 1 Empirical parameters to define power-on base pressure

M_∞	$C_1(C_T, M_\infty)$ for the following C_T :					$C_2(M_\infty, C_T)$ for the following C_T :	
	≤ 1.0	2.0	20	40	≥ 70	≤ 1.0	≥ 2.0
≤ 0.9	0.19	0.16	-0.06	0.02	0.0	1.24	1.24
1.0	0.19	-0.085	-0.06	0.02	0.0	1.28	1.37
1.25	0.19	-0.085	-0.01	0.02	0.0	1.28	1.47
1.65	0.19	-0.175	-0.06	0.04	0.0	1.28	1.70
2.0	0.19	-0.30	-0.20	0.02	0.0	1.28	1.90
2.5	0.19	-0.45	-0.23	0.01	0.0	1.28	2.30
3.0	0.19	-0.55	-0.22	-0.03	0.0	1.28	2.50
≥ 4.0	0.19	-0.65	-0.10	-0.04	0.0	1.28	2.7

appropriately fit the data of Fig. 2 and other experimental cases for high values of thrust. The method is defined by Eq. (8):

$$P_b/P_\infty = \left(\frac{T_j}{T_j^*}\right)^N \left[C_1(C_T, M_\infty) + C_2(M_\infty) \left(\frac{\text{RMF}}{1 + \text{RMF}} \right) \right] \times f\left(\frac{d_B}{d_r}\right) + 0.047(5 - M_\infty) \left[2\left(\frac{x_j}{d_B}\right) + \left(\frac{x_j}{d_B}\right)^2 \right] \quad (8a)$$

where

$$\begin{aligned} N &= \frac{12 - C_T}{11.0}, & 1.0 \leq C_T < 12 \\ &= 0, & C_T \geq 12 \\ &= 1, & C_T < 1.0 \end{aligned}$$

$C_1(C_T, M_\infty)$ and $C_2(M_\infty)$ of Eq. (8a) are found from Table 1 by linearly interpolating based on a given value of C_T and M_∞ . Also, for Mach numbers below about 1.5 it was found that T_j/T_j^* should have limiting lower values. This limiting lower value is defined by

$$\begin{aligned} \left(\frac{T_j}{T_j^*}\right)_{\min} &= 0.7 - (M_\infty - 1.2) \frac{(0.7 - T_j/T_j^*)}{0.3} & \text{for } 1.2 \leq M_\infty < 1.5 \\ \left(\frac{T_j}{T_j^*}\right)_{\min} &= 0.7 & \text{for } M_\infty < 1.2 \end{aligned} \quad (8b)$$

For values of Mach number above 1.5, T_j/T_j^* retains the value computed from Eq. (3). The boattail term $f(d_B/d_r)$ of Eq. (8a) was also found to be dependent on thrust coefficient. For low to moderate values of C_T on a boattailed configuration, $f(d_B/d_r)$ follows the form of Eq. (1). That is,

$$f\left(\frac{d_B}{d_r}\right) = \frac{3.5}{1 + 2.5(d_B/d_r)^2}, \quad C_T \leq 6.0 \quad (8c)$$

For higher values of C_T , Eq. (8c) is replaced by

$$\begin{aligned} f\left(\frac{d_B}{d_r}\right) &= 1 + \left(\frac{12 - C_T}{6}\right) \left[\frac{3.5}{1 + 2.5(d_B/d_r)^2} - 1 \right] & \text{for } 6 \leq C_T \leq 12.0 \\ f\left(\frac{d_B}{d_r}\right) &= 1, & \text{for } C_T > 12.0 \end{aligned} \quad (8d)$$

If the configuration has a flare, then $f(d_B/d_r)$ follows the form

$$\begin{aligned} f\left(\frac{d_B}{d_r}\right) &= \frac{3.5}{1 + 2.5(d_B/d_r)^2}, & C_T \leq 25 \\ &= 1 + \frac{75 - C_T}{50} \left[\frac{3.5}{1 + 2.5(d_B/d_r)^2} - 1 \right], & 25 < C_T \leq 75 \\ &= 1, & C_T > 75 \end{aligned} \quad (8e)$$

Equations (8c) and (8d) indicate that for lower thrust levels the base pressure is raised by a boattail, lowering base drag. However, for high values of C_T the base-pressure ratio is nearly independent of boattail, and the base-drag reduction comes purely from a base area reduction. Equation (8) reduces to the method of Brazzel at $\text{RMF} \leq 0.5$ but will give higher values than the Brazzel method for higher M_∞ . At transonic Mach numbers Eq. (8) can give values of P_b/P_∞ lower than the Brazzel method because Mach numbers as low as 0.9 have been included in Fig. 2 and Table 1, whereas the Brazzel method was originally derived for Mach numbers of 1.5 and greater. Also note that for C_T values greater than 12, the exit Mach-number dependence of Eq. (8) goes away. Whereas Eq. (8) is believed to be an improvement over the AP98 methodology⁸ and the Brazzel technique,^{1,2} Eq. (8) still lacks complete robustness in terms of nozzle exit geometry.

Another problem associated with the method outlined by Eqs. (1–8) and Fig. 2 for computing power-on base drag is the fact that for many users of the aeroprediction code information other than P_C may be available for a given rocket. Users would like the option for computing power-on base drag, given a value of thrust and either P_C/P_∞ , P_j/P_∞ , or M_j . Hence, for cases where thrust and P_C/P_∞ are known the process to calculate P_b/P_∞ is the same as Eqs. (1–7), except Eq. (8) is substituted for Eq. (1). If thrust and P_j/P_∞ are given, then from Eq. (7),

$$\text{RMF} = \frac{1}{2} \left[C_T - \left(\frac{d_j}{d_r} \right)^2 \frac{2}{\gamma_\infty M_\infty^2} \left(\frac{P_j}{P_\infty} - 1 \right) \right] \quad (9a)$$

Then, utilizing Eq. (2),

$$M_j = \sqrt{\frac{\text{RMF} \gamma_\infty P_\infty d_r^2 M_\infty^2}{\gamma_j P_j d_j^2}} \quad (9b)$$

Likewise, if thrust and M_j are known then utilizing Eqs. (2) and (7) we obtain

$$\frac{P_j}{P_\infty} = \frac{C_T + (2/\gamma_\infty M_\infty^2)(d_j/d_r)^2}{(2/\gamma_\infty M_\infty^2)(d_j/d_r)^2(1 + \gamma_j M_j^2)} \quad (10a)$$

RMF can then be computed from Eq. (2).

Finally, if thrust and P_C/P_∞ are given then utilizing Eq. (10) and isentropic flow relations we obtain

$$\frac{P_C}{P_\infty} = \frac{[C_T + (2/\gamma_\infty M_\infty^2)(d_j/d_r)^2] \{1 + [(\gamma_j - 1)/2] M_j^2\}^{\gamma_j/(\gamma_j - 1)}}{(2/\gamma_\infty M_\infty^2)(d_j/d_r)^2(\gamma_j M_j^2 + 1)} \quad (10b)$$

All terms in Eq. (10b) are known except M_j . M_j can be found by a numerical iterative solution of Eq. (10).

Of course, C_T is defined by

$$C_T = \frac{2T}{\gamma_\infty P_\infty M_\infty^2 A_{\text{ref}}} \quad (11)$$

C_{PB} , C_{AB} , and C_A are then obtained through use of Eqs. (5), (6), and (7), respectively.

A third alternative for rocket engine effects on base drag and total weapon performance is where you know nothing about the rocket engine, except you know you want to parametrically trade off power-on base drag as a function of weapon performance. For this option we define

$$C_{AB} = -K(C_{AB})_{\text{power off}} \quad (12)$$

where K varies from -1.5 to 2.5 . Although it is true that this alternative of base drag that allows a variation in C_{AB} from 1.5 to $-2.5C_{AB}$ is just an approximation based on no real rocket engine, the range of values are reasonable boundaries of what one should expect for power-on effects on base drag.

Base Bleed

Base bleed is an alternative considered for use, primarily in unguided projectiles, to decrease base drag. The concept works on the basis of burning a small amount of propellant in the base of a projectile. This burning generates an exhaust gas, which is typically subsonic and incompressible and raises the temperature and pressure in the base area, thus lowering the base drag. Figure 1b is an example of a base-bleed configuration taken from Ref. 3. There have been numerous references in the literature over the past 40 years or so that address the base bleed problem. Some of the more notable references are given by Refs. 10–20, in addition to Ref. 3. However, as noted by Danberg,³ many of these references investigated the effects of base bleed or base pressure in wind-tunnel tests where fairly high values of the nondimensional injection parameter were used. This parameter is defined by

$$I = \dot{m}_j / \rho_\infty V_\infty A_{\text{ref}} \quad (13)$$

and is the ratio of the mass flow out of the bleed exit to that in a stream tube of area equal to the cross-sectional area of the body. Many of Refs. 10–20 were for wind-tunnel tests where values of $I = 0.01$ to 0.04 were considered for cold air, whereas the practical case for projectiles is $I \cong 0.001$ to 0.005 with hot gas. These low values of I for projectiles are because only so much propellant can be carried in the projectile cavity (see Fig. 1), and if a high value of I is used the time over which the base-drag reduction occurs will be very short. A slower burn, lower velocity exhaust gas, and hence lower value of I is thus more practical, even though the optimum value of I is about 0.01 to 0.03 for minimum base drag based on the cold gas tests of Refs. 10 and 11.

Assuming values of I of 0.001 to 0.005 allows some simplifications in the base-pressure estimation process. The simplification occurs because for values of $I \leq 0.005$ the base pressure is approximately a linear variation with I . This linearity of base pressure for low values of I is shown by Refs. 11, 14, and 16.

Danberg³ used the conclusion of near linearity of P_b/P_∞ as a function of I for $I < 0.005$ to derive a semi-empirical relationship to predict base pressure. Because the purpose of including base bleed in the aeroprediction code (APC) is to allow application primarily to unguided projectiles and because the range of practical interest of base bleed for projectiles is fairly low, a slightly modified method of Danberg will be adopted for use in the APC. Danberg's method defines the base pressure as

$$P_b/P_\infty = (P_b/P_\infty)_{I=0} + \sigma I / (1 + \beta \sigma I) \quad (13a)$$

where

$$\sigma = \frac{d(P_b/P_\infty)}{dI} = (-5.395 + 0.0172T_j)M_\infty + (4.610 - 0.0146T_j)M_\infty^2 + (-0.566 + 0.00446T_j)M_\infty^3 \quad (13b)$$

$$\beta = 15.1 - 46.3(M_\infty - 0.71) \quad (13c)$$

T_j of Eq. (13b) must be in degrees Rankine. Also, if β is less than 2.6 it should be set to 2.6 according to Danberg. Also, an upper limit of P_b/P_∞ of 1.0 will be included in the modified Danberg theory. Notice that Eq. (13b) has some nonlinearity brought into the method through the second term. Danberg used a combination of computational fluid dynamics calculations for forebody wave and skin-friction drag, in conjunction with total axial force from ballistic range data, to back out the base axial-force term. Knowing C_{AB} , the base pressure for no base bleed can be calculated from

$$(P_b/P_\infty)_{I=0} = (\gamma_\infty M_\infty^2 / 2) C_{PB} + 1 \quad (14)$$

Equation (14) is then used as the first term of Eq. (13a). The present approach differs from Danberg's approach in that $(P_b/P_\infty)_{I=0}$ will be defined based on the present method in the APC.⁷ In this approach

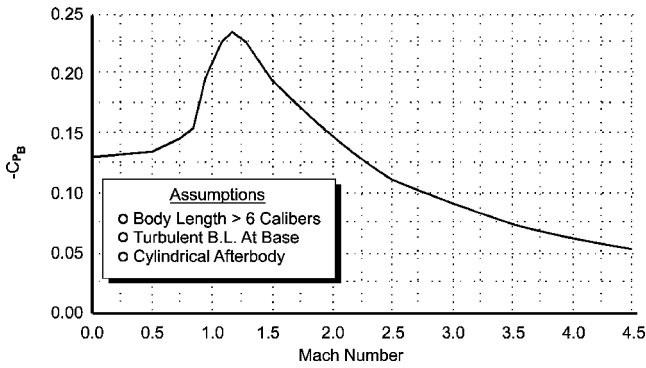


Fig. 3 Mean body-alone base-pressure coefficient used in AP98 (Ref. 8).

a mean base-pressure coefficient curve has been defined based on an extensive database taken over many years. This mean base-pressure coefficient curve is shown in Fig. 3.

Thus, for a given freestream Mach number one determines a value of $(P_b/P_\infty)_{I=0}$ from Eq. (14). Then for a given value of exit temperature T_j , freestream Mach number, and injection parameter I , the base pressure can be calculated directly from Eq. (13a). Base-pressure coefficient is then calculated from Eq. (4).

For the base-bleed methodology Danberg assumed that $P_j = P_B$ in his analysis. Hence, for base bleed we do not subtract the area of the exit from the axial-force calculations as we did for rocket motors [see Eq. (5)]. The base axial-force coefficient for base-bleed conditions is thus

$$C_{AB} = -C_{PB}(d_B/d_r)^2(d_B/d_r)^i$$

$$i = 0 \quad \text{for flare,} \quad i = 1 \quad \text{for boattail} \quad (15)$$

To summarize the new base-bleed methodology, which will be incorporated into the 2002 version of the APC, we will use a slightly modified method of Danberg, where base pressure is defined by Eqs. (13) and (14) and Fig. 3 and base axial force by Eq. (15). Equation (13a) requires an input value of freestream Mach number, exit temperature in degrees Rankine, and a value of the injection parameter I . For most accuracy I should be less than 0.005, but values of I as high as 0.01 can be assumed, but with larger errors in the prediction process.

Modified Base-Drag Prediction Model

The base-drag prediction model currently in use in the AP98 is described in Refs. 7 and 8. This model accounts approximately for the effects of Mach number, angle of attack, fin thickness, fin location, fin local angle of attack, power on/off, and boattail or flare. The method described in this paper will only affect the value of the power-on base-pressure coefficient of the body alone. It will be assumed that this new value of body-alone, base-pressure coefficient will replace that value currently used in the AP98. Then the effects of fins and angle of attack will be unchanged from that in Refs. 7 and 8.

Results and Discussion

The comparison of the theory and experiment will be separated into the base-bleed and power-on, base-drag predictions. The base-bleed results will be discussed first.

Base Bleed

There have been several experiments conducted to measure the effect on base pressure of bleeding a small amount of both cold and hot air into the base region of an ogive-cylinder configuration. The reader is referred to Ref. 9 for other validation results. The modified theory of Danberg will be compared to several of these and other results for validation.

The first set of results to be considered are those of Bowman and Clayden¹¹ and Reid and Hastings.¹⁰ They measured base pressure for various Mach numbers with cold air and an exit diameter ratio of

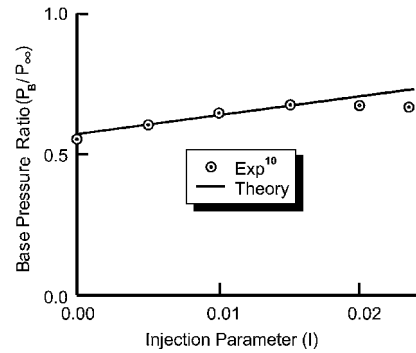


Fig. 4 Comparison of theory and experiment for base-pressure ratio at base-bleed conditions ($M_\infty = 1.58$, $d_j/d_r = 0.4$, $T_j = 520^\circ \text{R}$).

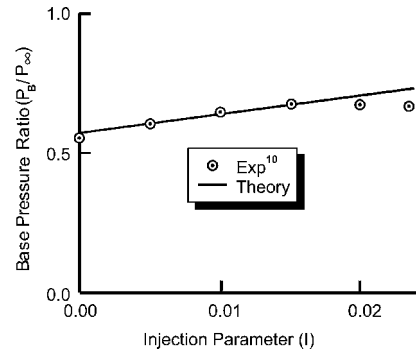


Fig. 5 Comparison of theory and experiment for base-pressure ratio at base-bleed conditions ($M_\infty = 2.0$, $d_j/d_r = 0.4$, $T_j = 520^\circ \text{R}$).

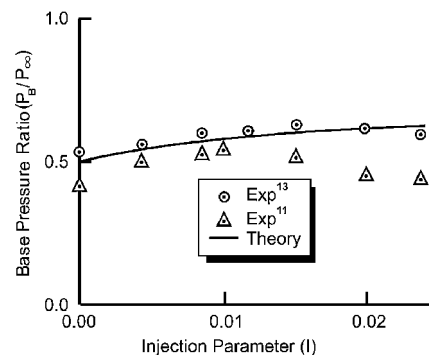


Fig. 6 Comparison of theory and experiment for base-pressure ratio at base-bleed conditions ($M_\infty = 2.5$, $d_j/d_r = 0.4$, $T_j = 520^\circ \text{R}$).

$d_j/d_r = 0.4$ (area ratio of 0.16). Figures 4–8 compare the theory to experiment. Figure 4 is for $M_\infty = 1.58$; Fig. 5 for $M_\infty = 2.0$; Fig. 6 for $M_\infty = 2.5$; Fig. 7 for $M_\infty = 3.0$; and Fig. 8 for $M_\infty = 3.88$. Figures 4 and 5 show excellent agreement with both the data of Bowman and Clayden¹¹ and Reid and Hastings¹⁰ at $M_\infty = 1.58$ and 2.0, respectively, for values of I as high as 0.02. At $M_\infty = 2.5$ (see Fig. 6) two sets of data are available. The theory matches the Ref. 14 data quite nicely, again to values of $I \cong 0.02$. On the other hand, the data of Bowman and Clayden¹¹ appears to be low for both this Mach number and Mach number 3.0 as well. It is suspected that the Ref. 11 data are low because of strut interference effects on base pressure for the higher-Mach-number conditions. Bowman and Clayden¹¹ pointed out that their strut was quite thick because of having the air pumped through the strut and into the base region.

The present authors found that with 89 base-pressure orifice measurements⁷ fins and struts do indeed affect the base pressure. This effect tends to lower P_b/P_∞ below the value it should be without the interference effect present. We were able to isolate the interference effect to a small region directly behind the fins or strut. When this region was area averaged over the entire base, a lower value of base-pressure coefficient was obtained and a higher value

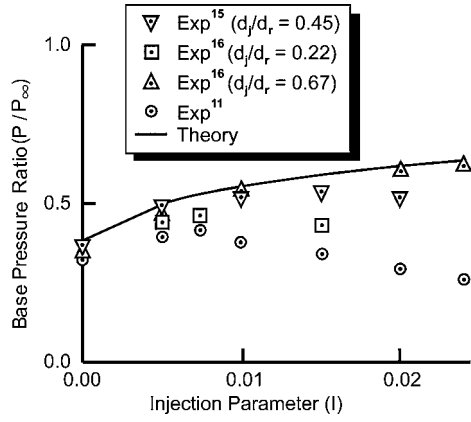


Fig. 7a Comparison of theory and experiment for base-pressure ratio at base-bleed conditions ($M_\infty = 3.0$, $d_j/d_r = 0.4$, $T_j = 520^\circ\text{R}$).

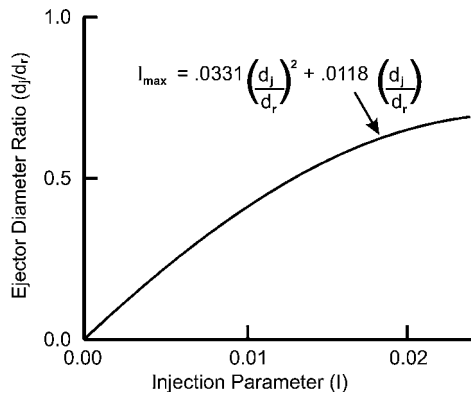


Fig. 7b Upper limit of I vs d_j/d_r for accurate values of P_B/P_∞ .

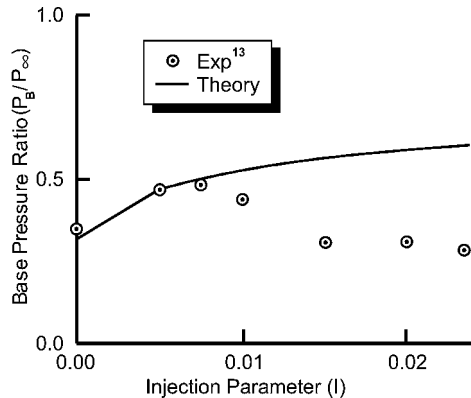


Fig. 8 Comparison of theory and experiment for base-pressure ratio at base-bleed conditions ($M_\infty = 3.88$, $d_j/d_r = 0.4$, $T_j = 520^\circ\text{R}$).

of base drag. With a large number of base-pressure taps, the interference effect of the strut would be eliminated. Reference 11 indicated the model diameter was only 1 in., and so it is suspected that not enough pressure taps were available to isolate the interference effect. This effect appears to be the highest at the higher Mach numbers.

Mach 3.0 results are given in Fig. 7a. Here, the theory is compared to the data of Ref. 11 as well as that of Ref. 16 for various size exit diameters of the injector. The theory matches the Ref. 16 data in an exceptional manner for large values of d_j/d_r (0.67) up to values of I of 0.025. However, for the smaller values of d_j/d_r of 0.22 theoretical computations are reasonable for I of 0.005 and less. However, for $d_j/d_r = 0.45$ the theory can be used up to values of I of 0.01. An empirical constraint, which can be used as an application guideline for the modified theory of Danberg, is shown in Fig. 7b based on the results of Fig. 7a. The equation shown in the figure

$$I_{\max} = 0.0331(d_j/d_r)^2 + 0.0118(d_j/d_r) \quad (16)$$

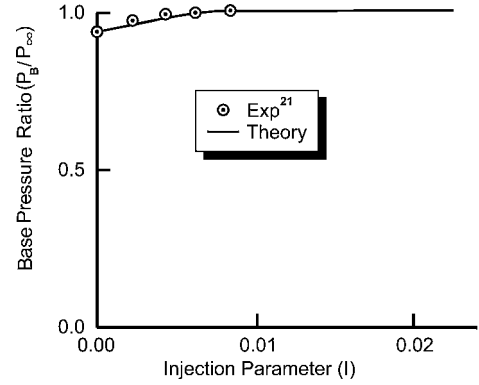


Fig. 9 Comparison of theory and experiment for base-pressure ratio at base-bleed conditions ($M_\infty = 0.71$, $d_j/d_r = 0.31$, $T_j = 2150^\circ\text{R}$).

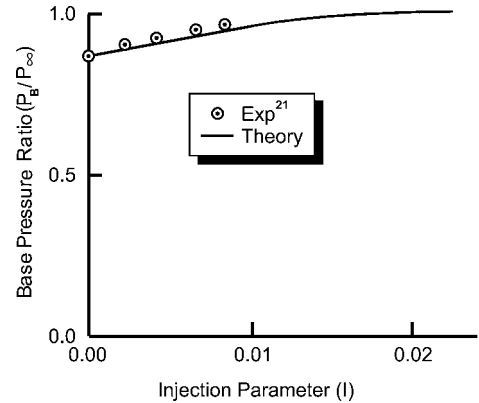


Fig. 10 Comparison of theory and experiment for base-pressure ratio at base-bleed conditions ($M_\infty = 0.98$, $d_j/d_r = 0.31$, $T_j = 2150^\circ\text{R}$).

gives the maximum value of I for a given value of ejector diameter ratio where accurate values of P_B/P_∞ can be expected from the theory. This equation is expected to be conservative for Mach numbers less than 3.0 and can be optimistic for Mach numbers greater than 3.0. This statement is based on the fact that as Mach number decreases, the value of I where accurate results of P_B/P_∞ can be expected increases for a fixed value of $d_j/d_r = 0.4$.

The last comparison of predicted base pressure with Mach number at room temperature conditions is shown on Fig. 8 for $M_\infty = 3.88$. The experimental data are taken from Ref. 13. As seen in the figure, acceptable accuracy can be obtained for values of I up to about 0.008.

Several cases were found where hot gas was used as the injectant. The first of these cases is taken from Ref. 21, and comparisons of theory and experiment at $M_\infty = 0.71$ and 0.98 are shown in Figs. 9 and 10, respectively. Temperature of the gas is 2150°R , and the ejector diameter ratio is 0.31. Comparison of theory to experiment is excellent for both Mach numbers, although data were only available for values of $I \leq 0.008$.

The next hot gas data are taken from Ref. 12. Bowman and Clayden¹² used argon heated to a range that varied from room temperature (520°R) to 9126°R at $M_\infty = 2.0$. The modified theory is compared to the Ref. 12 data for a T_j value for 5400°R , where $d_j/d_r = 0.2$ in Fig. 11. Recall from Fig. 7 that for values of $d_j/d_r = 0.2$ the maximum value of I where accurate results of the theory can be expected for a cold gas is approximately 0.0037. As seen in Fig. 11, for a hot gas this value of 0.0037 is too high by about a third. In other words, for a hot gas the limiting values computed for I_{\max} by Eq. (16) should be reduced somewhat. However, because the maximum value of base-pressure ratio occurs at approximately 0.0008 to 0.0022 for this case the theory is still reasonable for the practical case. That is because one would choose a value of I in the design process to give maximum values of P_B/P_∞ . Also, for a hot gas Eq. (16) should be modified according to

$$(I_{\max})_{\text{hot}} \cong \frac{2}{3}(I_{\max})_{\text{cold}} \quad (17)$$

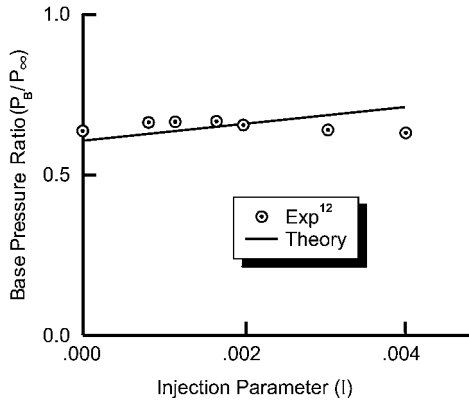


Fig. 11 Comparison of theory and experiment for base-pressure ratio at base-bleed conditions ($M_\infty = 2.0$, $d_j/d_r = 2.0$, $T_j = 5400^\circ\text{R}$).

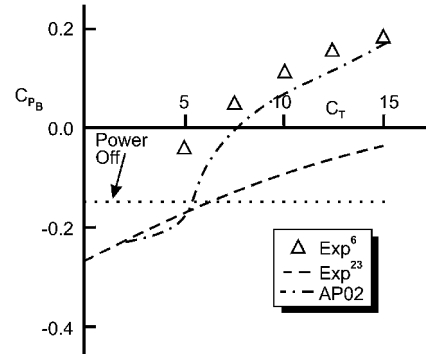


Fig. 15 Comparison of power-on, base-pressure coefficient prediction with experiment ($M_j = 2.5$, $M_\infty = 1.94$, $d_j/d_B = 0.75$).

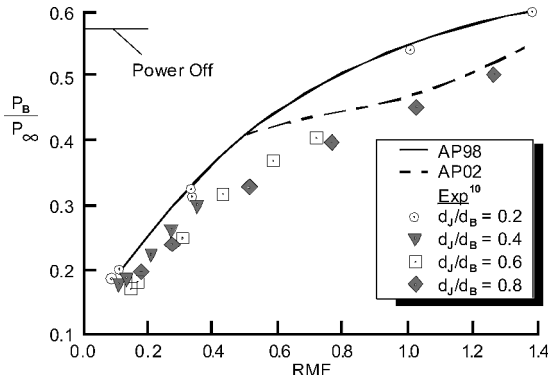


Fig. 12 Comparison of power-on, base-pressure prediction with experiment ($M_j = 2.0$, $M_\infty = 2.0$).

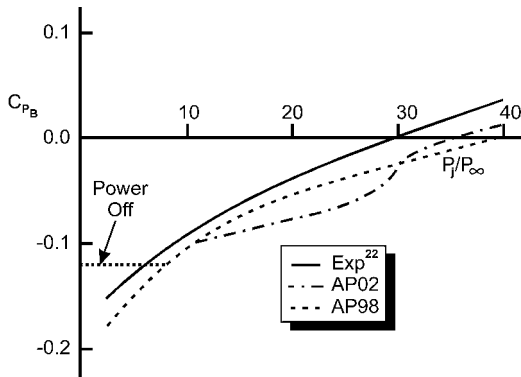


Fig. 13 Comparison of power-on, base-pressure coefficient prediction with experiment ($M_j = 1.0$, $M_\infty = 2.41$, $d_j/d_B = 0.5$).

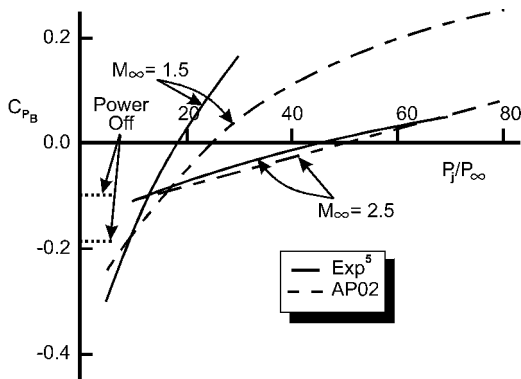


Fig. 14 Comparison of power-on, base-pressure coefficient prediction with experiment ($M_j = 1.0$, $d_j/d_B = 0.45$).

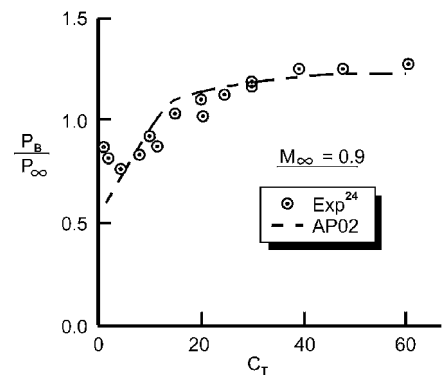
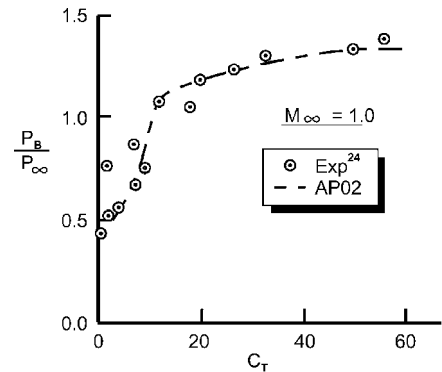
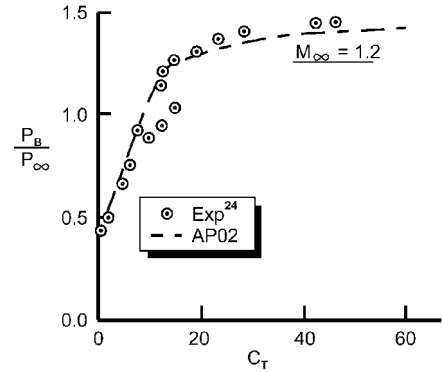


Fig. 16 Comparison of power-on, base-pressure coefficient prediction with experiment ($M_j = 2.7$, $d_j/d_B = 0.8$, 0.45 , $\theta_j = 20^\circ$ deg).

Power-On Base Drag for Rockets

The first case to compare the present predictions of power-on base pressure are results taken from Ref. 10 and correlated by Brazzel as a function of the jet momentum flux parameter RMF. These results, shown in Fig. 12, were for various jet to reference diameter ratios at $M_\infty = M_j = 2.0$. Also shown in Fig. 12 are the predictions of the Brazzel method (indicated by the AP98) for the low values of RMF computed from Eq. (1) for various values of RMF assuming

$\gamma_j = 1.4$ and $x_j = 0$. Because $M_j = 2$, $T_j/T_j^* = 0.67$, for Fig. 12. Also shown in Fig. 12 are the results for the improved method to be incorporated into the AP02 [see Eq. (8)]. As seen in Fig. 12, both the Brazzel technique and the AP02 method predict base pressure slightly high compared to the Ref. 10 data. This means base drag would be slightly low compared to the Ref. 10 experimental data.

The second case considered is taken from the data of Bromm and O'Donnell²² for a cylindrical afterbody configuration. The data are for sonic jet exit conditions at $M_\infty = 2.41$ and $d_j/d_B = 0.5$. Figure 13 compares the theory of AP02 to the experiment. Theoretical predictions give quite satisfactory comparisons to data with the base drag being somewhat high compared to data. The theory here is basically that of Brazzel and Henderson¹ up to P_j/P_∞ of about 10. Above P_j/P_∞ of 30, there is a slight improvement of the AP02 over the AP98 prediction, whereas for P_j/P_∞ less than 30 the AP02 gives slightly worse comparisons to data than the AP98.

The next case considered is taken from the data of Ref. 4. $M_\infty = 1.5$ and 2.5 cases are shown for the $M_j = 1.0$ and $d_j/d_r = 0.45$ conditions in Fig. 14. The AP02 gives excellent comparison to experiment at $M_\infty = 2.5$ and reasonable agreement at $M_\infty = 1.5$. The power-off base-pressure coefficient is noted for both the $M_\infty = 1.5$ case ($C_{PB} = -0.19$) and $M_\infty = 2.5$ case ($C_{PB} = -0.115$). This figure illustrates how power on can actually increase base drag over no power on at some conditions, whereas at other conditions base drag can be changed to base thrust.

The next case considered is taken from Ref. 23 and is for $M_j = 2.5$, $M_\infty = 1.94$, and $d_j/d_r = 0.75$. In addition to the experimental data of Ref. 23, the data of Ref. 5 are also shown in Fig. 15. The AP02 compares fairly well with the Ref. 5 data at

lower values of C_T and is in between the Ref. 5 and Ref. 23 data for higher values of C_T . Once again, the power-off, base-pressure coefficient is shown on Fig. 15, illustrating that at very low values of thrust coefficient power on increases base drag, whereas for higher values of C_T base drag is decreased.

The next three examples are taken from the experimental database of Rubin.²⁴ Rubin measured power on base drag in the transonic speed regime for cylindrical, flare, and boattail afterbodies at transonic Mach numbers. Figure 16 compares the semi-empirical predictions to the data of Rubin for the cylindrical afterbody at $M_\infty = 0.9$, 1.0, and 1.2. Experimental data were based on $M_j = 2.7$ and $d_j/d_B = 0.8$ and 0.45. A conical nozzle was used with $\theta_j = 20$ deg. The agreement between the experiment and theory at all three Mach numbers is reasonable. However, for $M_\infty = 0.9$ and $C_T < 4$ the experimental data show P_b/P_∞ increasing. The present theory will not predict the minimum base-pressure ratio. This increase in P_b/P_∞ will continue as C_T gets small until a maximum is reached at base-bleed conditions, after which P_b/P_∞ will decrease to its power-off value.

Figure 17 presents the comparison of theory and experiment for the boattailed afterbody case. Results for the same three freestream Mach numbers ($M_\infty = 0.9$, 1.0, and 1.2) are shown on the figure. The boattail angle is 6.35 deg, and the boattail length is 0.82 caliber. Again, reasonable agreement with experiment is seen except for $M_\infty = 0.9$ and 1.0 and for low values of C_T , where the minimum value of P_b/P_∞ has been reached.

Figure 18 presents the comparison of theory and experiment for the flare afterbody case. The flare angle is 6.54 deg, and its length is 1.34 caliber. Good agreement between theory and experiment is seen, except for $M_\infty = 0.9$ and $C_T < 6$, where the base pressure is seen to start increasing after a minimum has been reached.

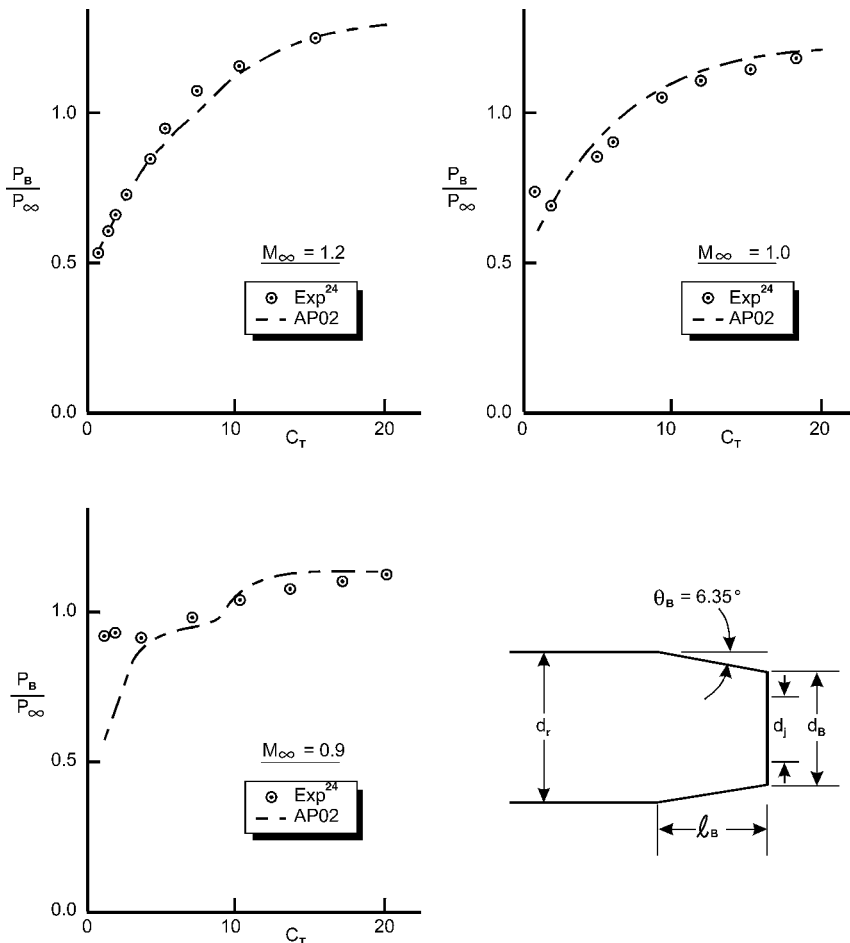


Fig. 17 Comparison of power-on, base-pressure prediction with experiment for boattail afterbody ($d_j/d_r = 0.45$, $\theta_j = 20$ deg, $\theta_B = 6.35$ deg, $\ell_B = 0.82$ cal, $M_j = 2.7$).

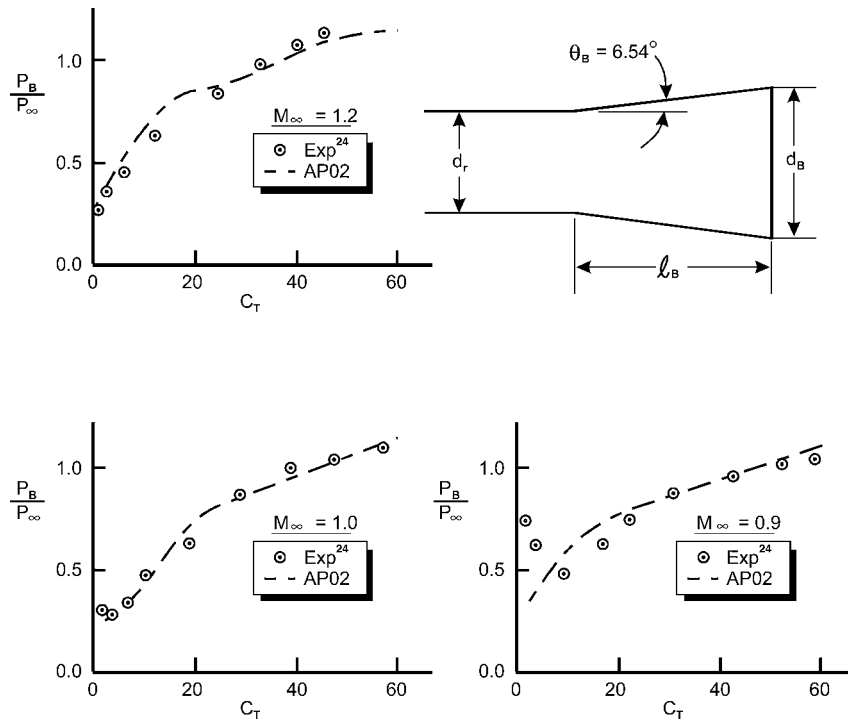


Fig. 18 Comparison of power-on, base-pressure prediction with experiment for flare afterbody ($d_j/d_r = 0.8$, $\theta_j = 20$ deg, $\theta_B = 6.54$ deg, $\ell_B = 1.34$ cal, $M_j = 2.7$).

Conclusions

To summarize the comparison to the experiment of the modified model of Danberg to predict base pressure at base-bleed conditions, the following conclusions were drawn:

1) The modified theory gave good agreement to cold gas experimental data for all practical values of the injection parameter and ejector diameter ratio and at all Mach numbers where data were found. These values are typically $I \leq 0.005$ and $d_j/d_r \approx 0.4$. The theory was seen to be accurate for many conditions outside the practical range of applicability.

2) A relationship was derived for cold gas conditions where the maximum value of I as a function of the ejector diameter ratio could be used with accurate values of base-pressure ratio expected. For hot gas conditions this cold gas upper limit was reduced by about one-third.

3) In general, the semi-empirical theory applicability range increases with decreasing Mach numbers (larger values of I allowed).

4) For limited hot gas comparisons of theory and experiment, it was seen that the theory gave acceptable agreement to the data. It was also seen that the optimum value of I is much lower than for cold gas conditions.

To summarize the power-on, base-drag prediction method for rockets, an improved semi-empirical method has been developed. The improved method is patterned after the method of Brazzel and Henderson¹ but has been modified significantly to make it more robust in terms of values of thrust coefficient allowed, freestream Mach numbers allowed, and afterbody geometries allowed. In comparing the new method to experimental data, it was seen to give reasonable comparisons to most databases. However, not all experimental data were consistent, and so part of the poor comparisons with some cases is believed to be experimental measurement problems. Although the new method has been validated with various types of afterbodies (boattail, flare, or cylinder), the method has not been validated at angle of attack or when fins were present. It is assumed that the change in base pressure caused by the presence of fins and angle of attack at power-off conditions can be applied directly to the power-on, base-pressure predictions.

Acknowledgments

The work described in this paper was supported by the Office of Naval Research through the Surface Weapons Systems Technology

Program managed at the Naval Surface Warfare Center, Dahlgren Division by Robin Staton. Tasking from this program was provided by Roger Horman and John Fraysse. The authors express appreciation for support received in this work.

References

- ¹Brazzel, C. E., and Henderson, J. H., "An Empirical Technique for Estimating Power-on Base Drag of Bodies-of-Revolution with a Single Jet Exhaust," *Conference on the Fluid Dynamic Aspects of Ballistics*, CP 10, NATO-AGARD, 1966, pp. 241-261.
- ²Moore, F. G., *Approximate Methods for Weapon Aerodynamics*, Vol. 186, Progress in Astronautics and Aeronautics, AIAA, Reston, VA, 2000, pp. 165-169.
- ³Danberg, J. E., "Analysis of the Flight Performance of the 155 mm M864 Base Burn Projectile," U.S. Army Research Lab., BRL-TR-3083, Aberdeen, MD, April 1990.
- ⁴Craft, J. C., and Brazzel, C. E., "An Experimental Investigation of Base Pressures on a Body of Revolution at High Thrust Levels and Freestream Mach Numbers of 1.5 to 2.87," U.S. Army Missile Command, Rept. RD-TM-70-6, Redstone Arsenal, AL, July 1970.
- ⁵Henderson, J. H., "An Investigation for Modeling Jet Plume Effects on Missile Aerodynamics," U.S. Army Missile Command, TR RD-CR-82-25, Redstone Arsenal, AL, July 1982.
- ⁶Deep, R. A., Henderson, J. H., and Brazzel, C. E., "Thrust Effects on Missile Aerodynamics," U.S. Army Missile Command, RD-TR-71-9, Huntsville, AL, May 1971.
- ⁷Moore, F. G., Hymer, T. C., and Wilcox, F. J., Jr., "Improved Empirical Model for Base Drag Prediction on Missile Configurations Based on New Wind Tunnel Data," U.S. Naval Surface Warfare Center, NSWCDD/TR-92/509, Dahlgren, VA, Oct. 1992.
- ⁸Moore, F. G., McInville, R. M., and Hymer, T. C., "The 1998 Version of the NSWC Aeroprediction Code: Part I-Summary of New Theoretical Methodology," U.S. Naval Surface Warfare Center, NSWCDD/TR-98/1, Dahlgren, VA, April 1998.
- ⁹Moore, F. G., and Hymer, T. C., "Improved Power-on, Base Drag Methodology for the Aeroprediction Code," U.S. Naval Surface Warfare Center, NSWCDD/TR-00/67, Dahlgren, VA, Oct. 2000.
- ¹⁰Reid, J., and Hastings, R. C., "The Effect of a Central Jet on the Base Pressure of a Cylindrical Afterbody in a Supersonic Stream," Royal Aircraft Establishment, Rept. Aero 2621, Farnborough, England, U.K., Dec. 1959.
- ¹¹Bowman, J. E., and Clayden, W. A., "Cylindrical Afterbodies in Supersonic Flow with Gas Injection," *AIAA Journal*, Vol. 5, No. 8, 1967, pp. 1524, 1525.
- ¹²Bowman, J. E., and Clayden, W. A., "Cylindrical Afterbodies at $M_\infty = 2$ with Hot Gas Ejection," *AIAA Journal*, Vol. 6, No. 12, 1968, pp. 2429-2431.

¹³Valentine, D. T., and Przirembel, C. E. G., "Turbulent Axisymmetric Near-Wake at Mach Four with Base Injection," *AIAA Journal*, Vol. 8, No. 12, 1970, pp. 2279, 2280.

¹⁴Mathur, T., and Dutton, J. C., "Base Bleed Experiments with a Cylindrical Afterbody in Supersonic Flow," AIAA Paper 95-0062, Jan. 1995.

¹⁵Sykes, D. M., "Cylindrical and Boattailed Afterbodies in Transonic Flow with Gas Ejection," *AIAA Journal*, Vol. 8, No. 3, 1970, pp. 588, 589.

¹⁶Kayser, L. D., "Effects of Base Bleed and Supersonic Nozzle Injection on Base Pressure," U.S. Ballistic Research Labs., Memorandum Rept. 2456, AD B 003442L, Aberdeen Proving Ground, MD, March 1975.

¹⁷Cortright, E. M., Jr., and Schroeder, A. H., "Preliminary Investigation of Effectiveness of Base Bleed in Reducing Drag of Blunt Based Bodies in Supersonic Stream," NACA RM E51A26, 1951.

¹⁸Murthy, S. N. B., Osborn, J. R., Parrows, A. W., and Ward, J. R. (ed.), *Base Flow Phenomena with and Without Injection: Experimental Results, Theories and Bibliography*, Vol. 40, Progress in Astronautics and Aeronautics, AIAA, New York, 1976, pp. 7-210.

¹⁹Kayser, L. D., Kuzan, J. D., and Vazquez, D. N., "Ground Testing for Base-Burn Projectile Systems," U.S. Ballistic Research Lab., BRL-MR-3708, Aberdeen Proving Ground, MD, Nov. 1988.

²⁰Badrinarayanan, M. A., "An Experimental Investigation of Base Flows at Supersonic Speeds," *Journal of the Royal Aeronautical Society*, Vol. 65, 1961, pp. 475-482.

²¹Ding, Z., Liu, Y., and Chen, S., "A Study of Drag Reduction by Base Bleed at Subsonic Speeds," First International Symposium on Special Topics in Chemical Propulsion: Base Bleed, Nov. 1988.

²²Bromm, A. F., and O'Donnell, R. M., "Investigation at Supersonic Speeds of the Effect of Jet Mach and Divergence Angle of the Nozzle upon the Pressure of the Base Annulus of a Body of Revolution," NACA RM E57E06, Aug. 1957.

²³Martin, T. A., and Brazzel, C. E., "Investigation of the Effect of Low Thrust Levels on the Base Pressure of a Cylindrical Body at Supersonic Speeds," U.S. Army Missile Command, RD-TR-70-11, Redstone Arsenal, AL, May 1970.

²⁴Rubin, D. V., "A Transonic Investigation of Jet Plume Effects on Base and Afterbody Pressures of Boattail and Flare Bodies of Revolution," U.S. Army Missile Command, Rept. RD-TR-70-10, Redstone Arsenal, AL, Oct. 1970.

M. S. Miller
Associate Editor